JOURNAL OF CATALYSIS **178,** 299–308 (1998)
ARTICLE NO. CA982152

The Synthesis and Characterization of Mesoporous High-Surface Area Ceria Prepared Using a Hybrid Organic/Inorganic Route

Daniela Terribile,* Alessandro Trovarelli,*[,1] Jordi Llorca,† Carla de Leitenburg,* and Giuliano Dolcetti*

**Dipartimento di Scienze e Tecnologie Chimiche, Università di Udine, via Cotonificio 108, 33100 Udine, Italy; and †Departament de Química Inorgànica, Universitat de Barcelona, Diagonal 647, 08028 Barcelona, Spain*

Received March 9, 1998; revised May 12, 1998; accepted May 12, 1998

The synthesis, characterization, and proposed formation mechanism of mesoporous high surface area ceria is described. It is shown that the reaction of cerium salts under basic conditions with ammonia in the presence of a cationic surfactant results in the precipitation of a gelatinous hydrous cerium oxide/surfactant mixture, which after drying and calcination gives pure, high surface area, fluorite-structured CeO_2. Although ceria does not show long range mesoscopic organization, it exhibits a broad arrangement of mesopores in the region 20–80 Å with a maximum located at around 35–40 Å. HRTEM detected very small crystalline CeO_2 particles with an approximate dimension of 20–50 Å. This ceria shows enhanced textural and thermal resistance features compared with ceria prepared by conventional routes. Surface areas in excess of 200 m^2/g are obtained after calcination at $T = 723$ K, which drop to ca 40 m^2/g after calcination at $T > 1173$ K; this highlights its better potential to operate as a catalyst support or promoter under medium/high temperature range. It is suggested that the cationic surfactant does not act as a true templating agent but as a surface-area enhancer by incorporation into the hydrous oxide and lowering of the surface tension of water in the pores during drying. © 1998 Academic Press

INTRODUCTION

Cerium oxide is currently being used as a promoter or support in several industrial catalytic processes and as a key component in the formulation of catalysts for the control of noxious emissions from mobile sources (1–2). The unique redox features of ceria, like the ability to shift between CeO_2 and CeO_{2-x} under reaction conditions, contribute to its success, especially when ceria is used as a component of the so called three-way catalysts (TWC).

In all commercial applications, stability of textural properties and resistance to sintering after aging play an important role. It has been recognized that thermal aging and loss of surface area are among the main causes of deactivation of ceria, especially in TWC (3). Various strategies have been pursued to develop ceria with enhanced textural and thermal properties: one is to support CeO_2 on inert carriers such as Al_2O_3, and another is the development of new methodologies for the preparation of cerium oxide with improved surface area and enhanced resistance to aging. Some of the approaches that have been recently applied to prepare powdered cerium oxide are homogeneous precipitation techniques with different precipitating agents and additives (4–7), hydrothermal synthesis (8), spray pyrolysis methods (9), inert gas condensation of Ce followed by oxidation (10), thermal decomposition of carbonates (11), microemulsion (12), and electrochemical methods (13). In all these cases, cerium oxide with surface area not exceeding 100 m^2/g at the lowest calcination temperatures ($T < 773$ K) were reported and only in a few cases were surface areas close to 200 m^2/g observed (5, 12). Generally, a severe loss of surface area is caused by thermal treatment of conventional CeO_2 at moderate temperatures ($973\ K < T < 1073\ K$) (14). This drop in surface area can be partially reduced if ceria is doped with rare earth or transition metals (15). Proprietary methods of preparation allow the stability range of ceria to be widened enough to reach temperatures of 1100 K without severe loss of surface area (16). It therefore appears that the preparation of high surface area, thermally resistant ceria may have great potential in the development of new redox catalysts.

An interesting approach to the preparation of mesoporous, high surface area materials was recently reported by scientists at Mobil for the preparation of a new family of mesoporous molecular sieves, designated M41S (17). This consists of using organic molecules, such as surfactants, as templating agents for the creation of a 3D array with regular structure. This approach has so far been applied to the preparation of transition metal oxides like ZrO_2 (18–21), TiO_2 (22), Nb_2O_5 (23), using different organic molecules as templating agents. Anionic, cationic, or amphoteric surfactants have been employed with success in the preparation of high-surface area materials. In a few cases, ordered pore structure was obtained after calcination (21, 23) but in the majority of cases the structure was observed to collapse upon calcination (18, 19). In addition in recent years, high

---

[1] Corresponding author. E-mail: trovarelli@dstc.uniud.it.

0021-9517/98 $25.00

surface area, mesoporous materials have attracted much attention because of their physical and chemical properties, which are significantly different from those of bulk materials (24).

As a part of a broader project aimed at preparing catalysts containing CeO_2 with improved textural and redox/catalytic properties, we are investigating the possibility of synthesizing mesoporous CeO_2 using organic molecules acting as “surface area enhancers” or “pseudo-templating agents.” The approach we are using exploits the interaction of hydrous cerium oxide with a cationic surfactant under basic conditions to promote exchange reaction with hydroxy surface groups. A preliminary account has recently appeared (25). Herein we report details of the preparation and the textural and morphological characterization of high surface area mesoporous ceria prepared using surfactants. In a forthcoming paper, details of the redox chemistry and catalytic redox properties of this cerium oxide will be presented.

EXPERIMENTAL

Synthesis of CeO_2

In a typical preparation, an aqueous ammonia solution (250 ml of NH_3, 25 wt%) was added dropwise over ca 2.5 h to a stirred solution of $CeCl_3 \bullet 7H_2O$ (Aldrich) containing cetyltrimethyl ammonium bromide (Aldrich) as surfactant (the solution was prepared with 11.2 g of $CeCl_3 \bullet 7H_2O$ and 9.4 g of surfactant in 550 ml of water, which represents a 1.2 molar ratio Ce/surfactant). Ammonia was added at 293 K and the pH of the solution varied from the initial value of 2.5 to a final value of 11.4. This caused the precipitation of hydrous cerium oxide as a gelatinous pale yellow solid. After precipitation, the slurry was stirred for one further hour and then the mixture was sealed in a glass vessel and placed in a thermostatic bath at 363 K for 90 h under continuous stirring. The mixture was then cooled at room temperature and the precipitate filtered and washed, first with water (1.5 liter) and then with acetone (500 ml). This procedure was used in order to better remove the surfactant not incorporated within the oxide. The resulting yellow powder was dried at 333 K for 24 h in an oven and calcined in a tubular furnace (ID 50 mm, length 900 mm) for at least 2 h at different temperatures (623–1273 K, with a heating rate of 10 K/min). The calcination was carried out with an air flow (0.2 liters/min, STP) passing over the sample placed in a quartz dish inside the furnace. The yield, calculated by assuming the composition reported in Table 1 was 93.1%. Similar syntheses were performed by varying reaction pH (9–13), the cerium salt (nitrate vs chloride, Ce^{3+} vs Ce^{4+}), Ce/surfactant ratio (0.6–1.25), reaction time (0–90 h), and the surfactant (we used alkyltrimethylammonium bromides or chlorides with a carbon chain length varying from 14 to 18 carbon atoms). Cerium oxide prepared using this procedure (hereafter called HSA CeO_2) was compared to CeO_2 prepared by conventional precipitation with ammonia (CVZ CeO_2) by using the process described above without the addition of surfactant.

TABLE 1

Stoichiometry of Ce-surfactant before Calcination: CeO_x-$(ONC_{19}H_{42})_n \bullet yH_2O$[a]

pH	n	y	SA (m^2/g)[b]
9	0.035	0.2	93
11.4	0.06	0.4	195
13	0.12	0.8	231

[a] Reaction time 90 h, $T = 363$ K. Samples were dried at 343 K for 15 h.

[b] Surface area after calcination at 723 K.

Characterization

The textural properties and porosity of cerium oxide were studied by adsorption of nitrogen at 77 K with a Carlo Erba Sorptomatic 1900 instrument. Surface areas were calculated by the BET method and pore size distribution was analyzed using the desorption branch of the isotherm and the Dollimore/Heal method. Thermal decomposition of the solid was studied by thermogravimetry (TG/DTA) using a Netzsch STA equipment. Samples (ca 200 mg) were heated in an alumina crucible from room temperature to 1473 K at a rate of 10 K/min.

Sample microstructure was investigated by scanning electron microscopy (SEM) as well as by conventional and high resolution transmission electron microscopy (HRTEM). SEM was carried out on a Leica LC-360 instrument using an accelerating voltage of 10 kV. Samples of the materials were mechanically deposited on the holders and subsequently gold coated to reduce charge buildup. High resolution transmission electron microscopy (HRTEM) was performed on a Philips CM-30 instrument using axial illumination by 300 kV electrons. Samples of the catalysts were suspended in methanol and transferred to copper grids covered with perforated carbon film as they were dipped into the suspensions. A top entry double tilt specimen holder was used in all cases.

Powder X-ray analysis was carried out with a Siemens powder diffractometer using Cu-Kα radiation ($\lambda = 1.5418$ Å) by placing samples in aluminum sample holders and collecting the diffractogram over a 14-h period from $2\Theta = 20$–75 with a 0.02° step size. For low angle X-ray diffraction a Philips PW1830 instrument with Ni-filtered Cu-Kα radiation was used with a position sensitive detector (Anton Paar K. G.). FT-IR spectra were collected using a Digilab FT-40 spectrometer. Samples were mixed with KBr and pressed into a wafer for measurements.

RESULTS

Preparation and Characterization of CeO_2

The reaction of cerium salts (either chloride or nitrate) under basic conditions with ammonia at room temperature results in the precipitation of gelatinous, hydrous cerium oxide. If the reaction is conducted in the presence of cationic surfactants (i.e., alkyltrimethylammonium salts), hydrous cerium oxide can incorporate the organic molecule by exchange with surface OH groups. This approach follows the observation that hydrous oxides can exchange either cations or anions, depending on the pH of the medium. If the pH is higher than that of the isoelectric point of hydrous cerium oxide, incorporation of cationic surfactants takes place, according to the equilibrium depicted below:

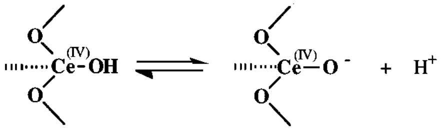

SCHEME 1

The pH of the isoelectric point for hydrous cerium oxide is in the range 6.75–8, depending on the environment (concentration, presence of different ions) (26), and under highly basic conditions ($pH > 9$), the equilibrium shifts to the right with a net negative charge on the surface. The inorganic/organic mixture that is formed by reaction of hydrous cerium oxide with the alkylammonium salt under these pH conditions can be isolated from the reaction medium by filtration and washing. Even after thorough washing, the presence of surfactant is clearly observed by FT-IR, TG, and elemental analysis. Figure 1a shows the IR spectra in the region 2000–4000 cm^{-1} of CeO_2 prepared by varying the time of reaction between the hydrous oxide and the surfactant at a pH of 11.4. The IR absorption bands in the region of 2800–2900 cm^{-1} are typical of the C-H stretching mode of hydrocarbons. These bands are easily assigned to the presence of the surfactant hydrocarbon chain. Band intensity is dependent on reaction time; the longer the time the more intense the band. The surface area of the resulting cerium oxide also increases (Fig. 1b). It appears that the maximum extent of reaction occurs within ca 90 h. Longer reaction times do not produce any appreciable modification of C-H vibration intensity and, correspondingly, the textural properties of the final material are not changed. A complete IR spectrum of the materials collected after drying is reported in Fig. 2, which also shows the effect of pH on surfactant incorporation. Residual water and a hydroxy group are detected with a large band around 3500 cm^{-1}, corresponding to O-H stretching frequency, and broad bands at 1600 cm^{-1}, due to the bending vibrations of associated water. Additional bands at around 1450–1500 cm^{-1} and 720 cm^{-1} are assigned to the bending vibrations of the C-H bond of methylene groups (scissoring and rocking vibrations). As expected, infrared absorption bands due to the presence of hydrocarbon became more intense as pH increased, indicating substantial incorporation of the surfactant into the sample. Another series of strong bands is located around 1000–1110 cm^{-1}. The intensity of these bands is dependent on the surface area being stronger on freshly prepared ceria and weaker after calcination. They are most probably associated to the formation of "carbonate-like" species on the ceria surface, which decompose after treatment at high temperatures (1).

The elimination of weakly adsorbed water and surfactant takes place at temperatures in the 400–700 K range. This is

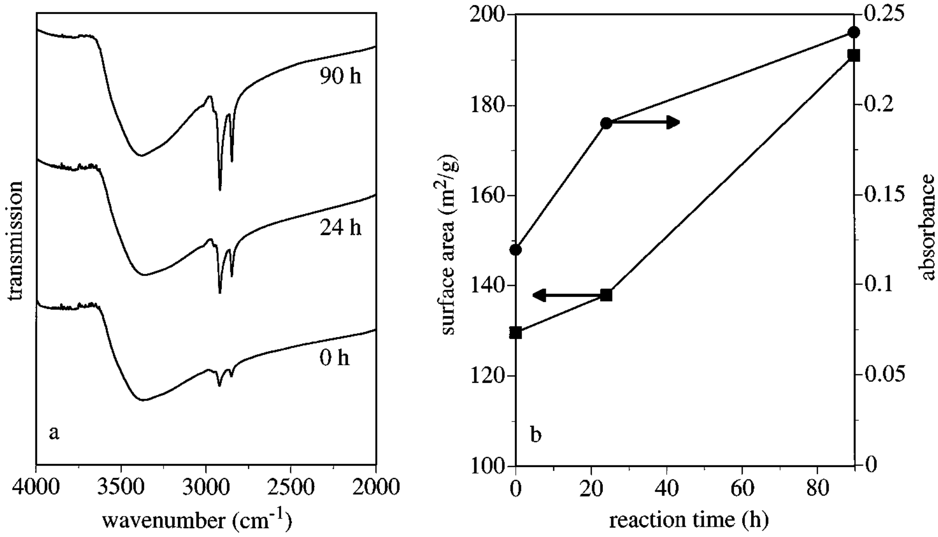

FIG. 1. (a) FT-IR spectra of dried HSA CeO_2 prepared at different reaction times at 363 K; (b) intensity of the C-H absorption bands of incorporated cetyltrymethylammonium salt in dried ceria samples and surface area of the resulting material calcined at 723 K.

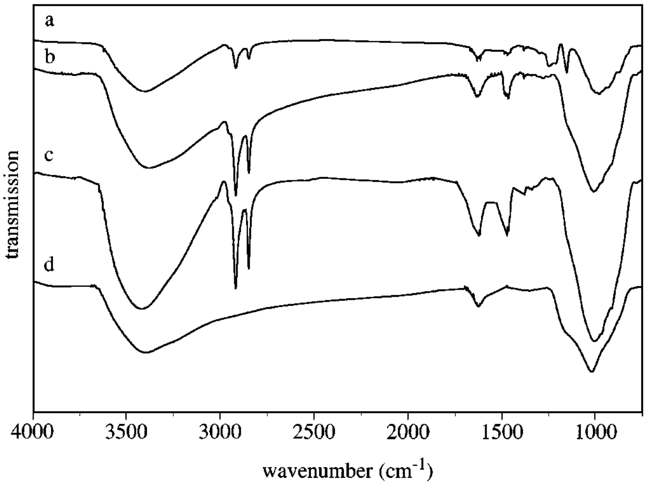

FIG. 2. FT-IR spectra of dried HSA CeO_2 prepared by varying the pH of reaction: (a) pH 9, (b) pH 11.4, (c) pH 13; (d) FT-IR spectra of HSA CeO_2 calcined at 923 K.

confirmed by combined TG/DTA, FT-IR, and elemental analysis. The FT-IR spectrum of the material after calcination at 923 K is shown in Fig. 2d. The vibrations belonging to C-H groups are completely lost and only residual OH groups are left on the surface. The loss of water and organics is also detected by TG/DTA; a representative profile is reported in Fig. 3. A weight loss ranging from 8 to 16% is calculated from TG measurements in the range 400–700 K for all samples examined. In the same temperature range, a series of exothermic peaks is observed in the DTA profile. It is suggested that elimination of organics through oxidation generates an exothermic reaction whose peak covers the peak originating from the endothermic desorption of water. The other exothermic peak centered at around 1000 K, not associated with weight loss, is due to the crystallization of ceria.

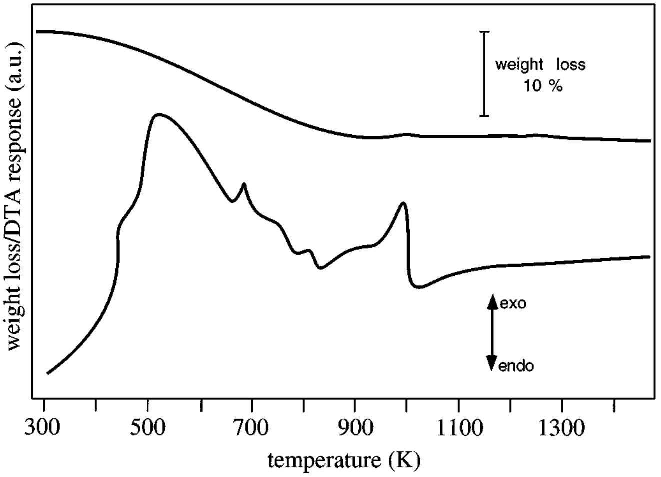

FIG. 3. A representative simultaneous TG-DTA curves for dried HSA CeO_2 in static air.

The composition of the "as synthesized" material after filtration and drying was checked by C,N,H elemental analysis. The C/N atomic ratios of the material is consistent with the surfactant remaining intact during the synthesis. The dried material can be formulated as $CeO_x(O\text{-}NC_{19}H_{42})_n \bullet yH_2O$, if cetyltrimethylammonium salt is used. Residual chlorides or bromides, originating from the surfactant, are not detected in the dried samples, as checked by the reaction of the dissolved material with a solution of $AgNO_3$. Carbon is not detected in the samples at calcination temperatures higher than 623 K, while a residual carbon (0.19 wt%) remains on the sample at this temperature. In Table 1 the values of n and y are calculated from elemental analysis combined with TGA. It is shown that, in conformity with the equilibrium described above, increasing the pH of the reaction results in a higher loading of the surfactant, incorporated by exchange in the presence of a high number of hydroxy M-O$^-$ groups. This results in a corresponding increase of the surface area, which reaches values exceeding 230 m^2/g after calcination at 723 K. The maximum is reached at $n = 0.12$, corresponding to incorporation of one molecule of surfactant every eight/nine cerium atoms. Bearing in mind that for a surface area of 200 m^2/g approximately one out of three cerium atoms is exposed (27), this means that we have ca. one mole of surfactant every three surface cerium atoms. The value is slightly lower than that reported in the case of synthesis of ZrO_2 using surfactants (18). In that case, the overall exchange capacity of hydrous zirconium oxide was one mole of surfactant every three or four zirconium atoms, which is a value close to the literature value for the cation exchange capacity of ZrO_2 (26).

Careful observation of the colors of the solution/slurry during synthesis is another interesting probe to check for the formation of intermediates. During the process, we observed changes in the color as the pH was raised and surfactants were added. The initial $Ce(NO_3)_3$ or $CeCl_3$ solution is clear and it remains colorless after the addition of surfactant. It is only when the pH is raised by the addition of ammonia that the solution turns opaque with a deep violet color. In a few hours, before sealing the mixture, the slurry turns brown and then light yellow, remaining light yellow for the entire reaction time (90 h), as well as during drying and calcination. By performing the reaction under identical conditions of concentration, pH, and temperature, but without the addition of the surfactant, the colors evolve in a different way. The slurry during reaction remains violet/brown even after filtration and washing, turning light yellow only after drying. These observations (see discussion section) indicate that the surfactant promotes the formation of yellow hydrous oxide before calcination.

Structural and Morphological Studies

Structural and textural-morphological investigations were carried out by powder X-ray diffraction (conventional and low-angle), coupled with scanning and high-resolution transmission electron microscopy. This was done in order to evaluate: (i) whether the incorporation of cationic surfactants gives rise to a long-range 3D ordered structure, as reported for various oxides containing transition metal, at least before calcination and (ii) whether this leads to enhancement of the textural properties of ceria. There is a broad consensus that the preparation of mesoporous materials results from a self-assembly process involving electrostatic interaction between positively charged quaternary ammonium salts and inorganic anions acting as framework precursors. Using this and similar approaches involving, for example, organometallic precursors it was possible to prepare transition metal oxides with a regular three-dimensional structure (23). However, most of these attempts were not successful in generating an oxide which could maintain a stable mesoporous structure upon removal of the organic moiety. In the case of zirconium, the partial degree of ordering which was observed in the dried material as a consequence of the introduction of the surfactants (18) was lost following thermal treatments. Nevertheless, the procedure enabled materials with very high surface area to develop even after calcination.

The low-angle X-ray diffraction pattern of the "as-synthesized" ceria did not show intense reflections at low 2Θ values. Only one weak peak was observed (Fig. 4), corresponding to a value of d-spacings of 20.5 Å. This value is not dependent on the chain length of the incorporated alkyltrimethylammonium cation, indicating that there is no long-range order in the structure, or at least that the order is limited to a few regions.

The lack of a long-range ordered structure is also confirmed by microscopy studies. Figure 5 shows a representative HRTEM image of fresh "as synthesized" ceria prepared using surfactants. As can be seen, there are already well-defined very small crystallites for most particles which can be indexed as those of cerium (IV) oxide with the cubic fluorite structure by the selected area electron diffraction pattern. This indicates that the precipitate from the reaction of cerium chloride/nitrate with ammonia, following the incorporation of surfactant, already displays the pattern of a Ce(IV) compound, which is in agreement with the light yellow color of cerium hydrous oxide observed during reaction. The microstructure, crystal size distribution, and morphology of the material is very homogeneous and similar to those exhibited by samples prepared without the incorporation of surfactants. In all cases, the atomic assembly as revealed by HRTEM is ordered only at a microdomain level, and in some regions is highly disordered, and pores are irregularly spaced and broadly distributed in size. The similarities between crystallite dimensions obtained by HRTEM (20–50 Å) on the fresh material, and those calculated assuming spherical particles of approximately 180–230 m^2/g (values measured for ceria after thermal treatment at 623–723 K), ranging from 36 to 46 Å, indicate that no aggregation occurs upon calcination of samples at low temperatures.

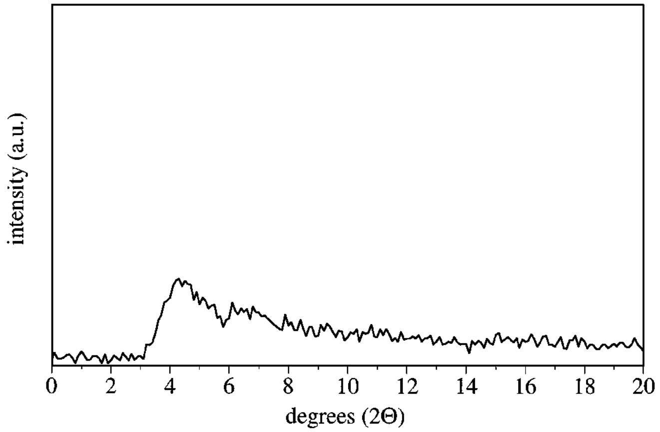

FIG. 4. A representative low-angle powder X-ray diffraction profile for dried HSA CeO_2.

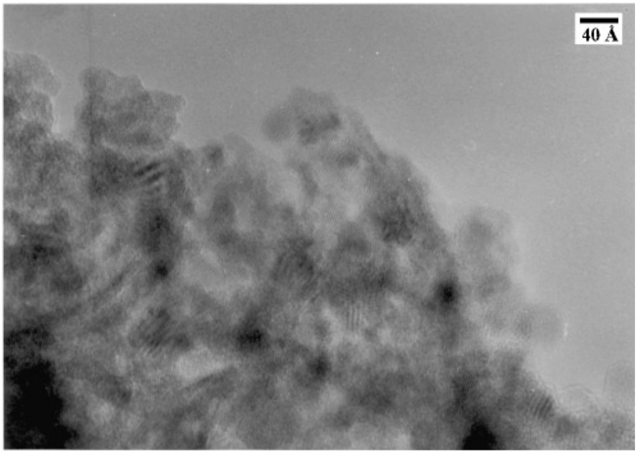

FIG. 5. High-resolution TEM image of fresh HSA CeO_2 calcined at 723 K.

The SEM micrographs of mesoporous ceria prepared with and without surfactants are illustrated in Figs. 6a and 6b, respectively. Both samples show the typical feature of an agglomerated powder. However, the sample synthesized through the incorporation of surfactants exhibits a considerably large degree of porosity, whereas the microstructure of the sample prepared without surfactants indicates a higher degree of agglomeration.

BET surface areas obtained after thermal treatment under air at increasing temperatures are reported in Fig. 7. Every experimental point is obtained by leaving the sample for 2 h at the calcination temperature indicated (heating rate 10 K/min) under air flow in a tubular furnace. Comparison with similar data obtained using CVZ CeO_2 or taken from the literature show that the textural features of HSA CeO_2 are superior to those of conventional CeO_2,

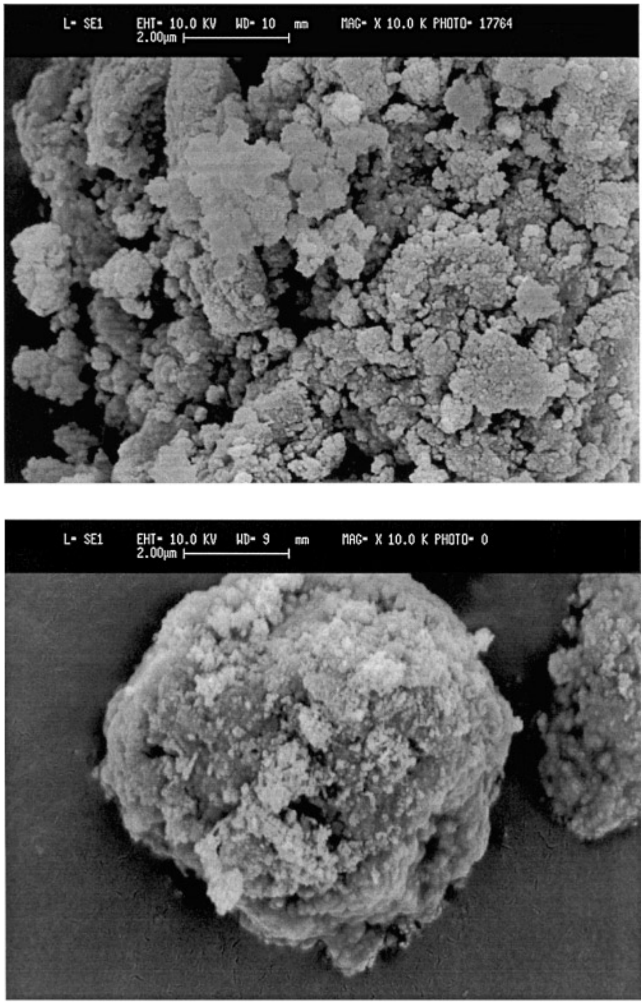

FIG. 6. Scanning electron micrographs of a fresh CeO_2 sample calcined at 723 K prepared with (upper) and without (lower) surfactants.

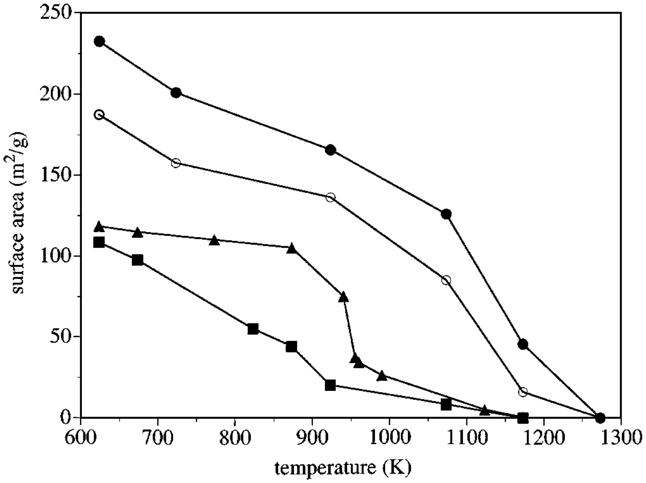

FIG. 7. Surface areas obtained by calcination of HSA CeO_2 at various temperatures for 2 h. The maximum (●) and minimum (○) value refer to results obtained following several different preparation (ca 60) at the following conditions: pH 11.4, Temp. 363 K, time 2–4 days; Ce/surf. ratio 1/0.8, chain length of surf. 14–18 carbon atoms. Surface area of conventionally prepared CeO_2 (■) and data taken from the literature, Ref. (14) (▲).

particularly in the temperature range 900–1200 K, which is of practical importance for ceria-containing TWC applications. With conventional ceria, a drop in surface area is generally observed around 900 K, which brings the specific area to a few square meters per gram. With HSA CeO_2 the surface area at 1073 K is stable at a value of ca 100 (see Table 2) for at least 40 h and drops to ca 40 m^2/g at 1173 K. TEM measurements indicate that the loss in surface area at high temperatures is due to an increase in the size of crystallite domains from a value of 2–5 nm, observed after calcination at 723 K to 30–100 nm, observed after calcination at 1273 K (Fig. 8). This is also consistent with X-ray powder diffraction data of HSA CeO_2 calcined at increasing temperatures, reported in Fig. 9. The profiles show the typical features of a fluorite-structured material (fcc with $a = 0.541$ nm). The sintering of HSA CeO_2 crystallites is particularly evident in the temperature range 1073–1273 K with a narrowing of the diffraction peaks, indicating an increase of particle dimensions. This is also in agreement with the loss of surface area observed following calcination at temperatures higher than 1173 K.

The other data reported in Table 2 indicate that the surface area depends on the chain length of the surfactant used, being higher with surfactants having 14 to 16 carbon atoms (runs 2, 3, and 5), while it is not strongly dependent on the ratio Ce/surf we have used (compare runs 3, 10, and 11). By keeping in mind that approximately one mole of surfactant is incorporated for every eight/nine cerium atoms, the

TABLE 2

Textural Properties of CeO_2 Samples Obtained by Varying Reaction Parameters[a]

Sample #	Calcination temp. T (K)	Calcination time (h)	pH	Ce/surf.	Chain length (number C atoms)	Surface area (m^2/g)
1	723	2	11.4	1/0.8	-	94
2	723	2	11.4	1/0.8	14	200
3	723	2	11.4	1/0.8	16	201
4	623	2	11.4	1/0.8	16	232
5	723	2	11.4	1/0.8	18	169
6	723	2	9	1/0.8	16	93
7	1173	2	9	1/0.8	16	36
8	723	2	13	1/0.8	16	231
9	1173	2	13	1/0.8	16	<1
10	723	2	11.4	1/1	16	191
11	723	2	11.4	1/1.5	16	192
12	1073	2	11.4	1/0.8	16	126
13	1073	5	11.4	1/0.8	16	112
14	1073	20	11.4	1/0.8	16	100
15	1073	40	11.4	1/0.8	16	96

[a] Reaction time 90 h, $T = 363$ K. Samples were dried at 343 K for 15 h.

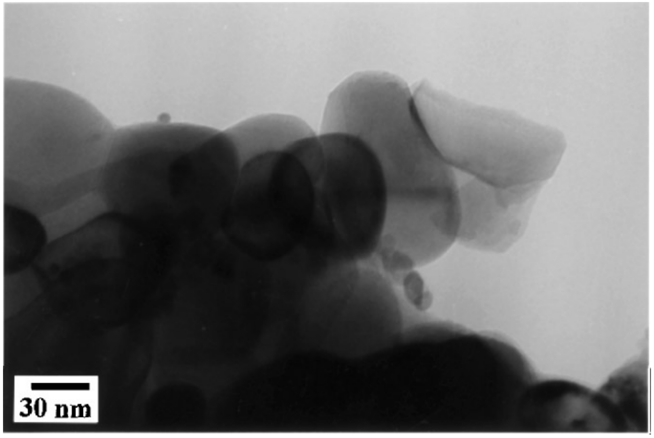

FIG. 8. TEM image of HSA CeO_2 calcined at 1273 K for 2 h.

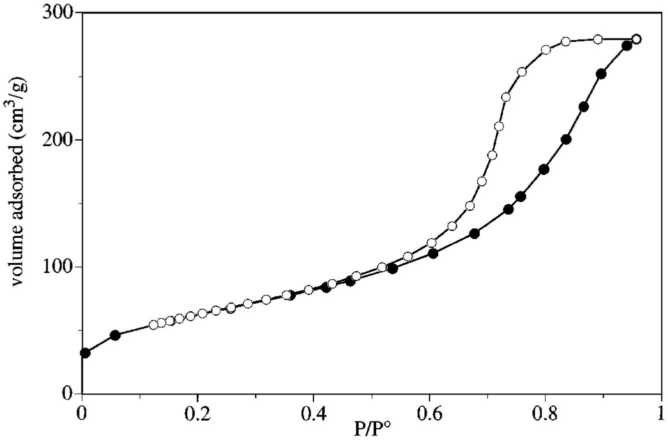

FIG. 10. A representative N_2 adsorption/desorption isotherm for mesoporous ceria (BET surface area 232 m^2/g).

amount used is well above that required, and no variation is expected in this concentration range. Overall, the most effective parameter is the pH of the reaction medium, which effectively shifts the equilibrium by increasing the number of surface OH groups. However, while by increasing the pH, an increase of the surface area of the fresh material is always observed; a better thermal resistance is evidenced for ceria prepared in the range of pH 9–11.

The nitrogen adsorption/desorption isotherm measured for a representative sample of HSA CeO_2 (surface area 232 m^2/g) is reported in Fig. 10 and can be classified as a type IV isotherm, typical of a mesoporous material (similar shapes are obtained in the isotherms of all samples investigated). The shape of the curve, in agreement with results from transmission electron microscopy studies, indicates the absence of a narrow pore size distribution, as suggested by the lack of the typical step in the adsorption isotherm which is observed with ordered mesoporous materials. According to IUPAC classification, the hysteresis loop is type H2 indicating a complex mesoporous structure. The pore size distribution calculated from the desorption branch is reported in Fig. 11 for HSA CeO_2 calcined at various

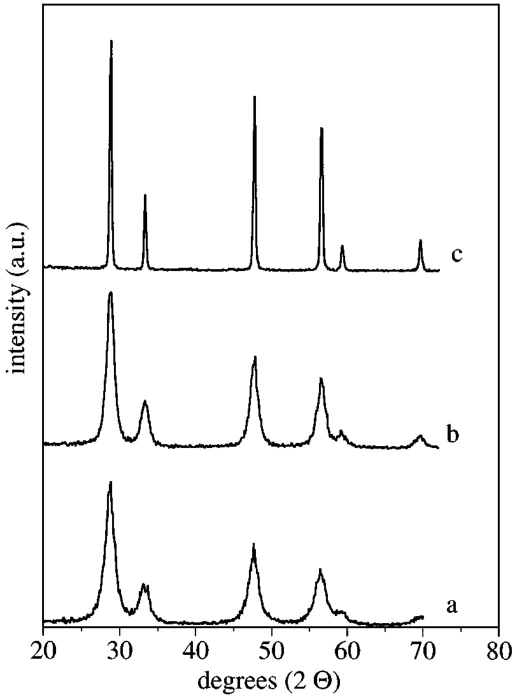

FIG. 9. X-ray diffraction patterns for HSA CeO_2 calcined at (a) 923 K, (b) 1073 K, and (c) 1273 K.

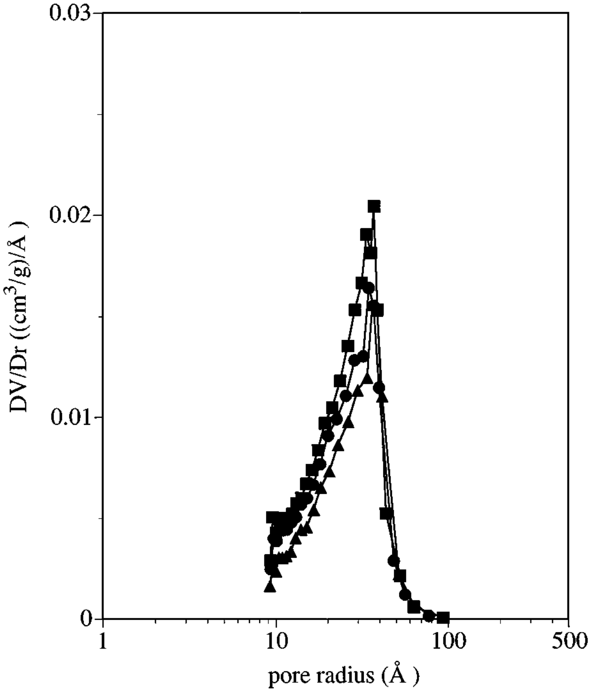

FIG. 11. Pore size distribution of HSA CeO_2 calcined at increasing temperatures: (■), 673 K; (●), 923 K; (▲), 1073 K, showing the pore opening range centered at ca 35 Å pore radius.

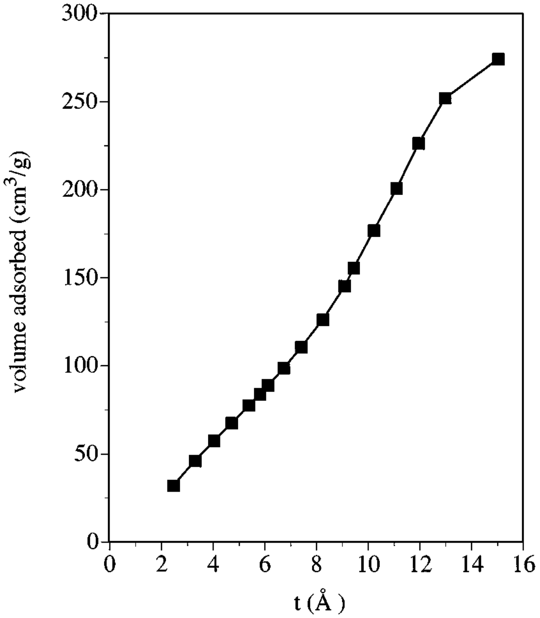

FIG. 12. Representative "t-plot" of HSA CeO_2.

temperatures. It may be observed that the material has a pore distribution covering the range 10–80 Å with a maximum at around 35 Å, which is not dependent on the calcination temperature from 723 to 1073 K. By increasing the calcination temperature only a variation in the amount of total pore volume is observed but there is no change in the distribution of pore dimensions, indicating a moderate sintering which takes place without modification of the pore radius. In accordance with the observed lack of long range order, we did not observe any variation of the pore size distribution curve on changing the chain length of the surfactant used. The "t-plot" obtained from the adsorption branch of the isotherm is reported in Fig. 12. The initial slope leads to a value of 224 m^2/g (obtained from the relation $t(\text{Å}) = \{13.99/[\log(p_0/p) + 0.034]\}^{1/2}$ (28)) in excellent agreement with the value of 232 m^2/g calculated using the BET method. This indicates an absence of micropores below ca 9 Å. The low value of the BET constant c in all samples ($50 < c < 120$) is further indication of an absence of microporosity.

DISCUSSION

The results presented here show no evidence that cerium oxide in the presence of surfactants forms an ordered templated oxide, although very high surface area develops after calcination. In the formation of an ordered 3D structure, it is well accepted that the organization of surfactants into various configurations is directed by the electrostatic interactions with charged inorganic species whose charge, coordination, and geometry are in turn governed by pH, temperature, concentration, counterions, and solvent. The ion pairs formed between inorganic and organic species organize into liquid crystal arrays and finally oxide condensation place. Thus any variation in the nature and charge of ions during the process could lead to a modification of the final material. From the results presented here it can be inferred that the surfactant interacts with hydrous Ce(IV) oxide which has already formed during the precipitation/reaction stage. This implies that oxidation of Ce^{3+} takes place during the reaction of $Ce(NO_3)_3$ with ammonium hydroxide. The driving force for the oxidation of Ce^{3+} is related to the basicity of the reaction medium. According to the definition of basicity, Ce^{3+} can be regarded as a Lewis base while Ce^{4+} is a Lewis acid. Basic solutions, therefore, favor the formation of Ce^{4+}. This is quantified by the following equilibrium:

$$Ce^{3+} + H_2O \Leftrightarrow Ce(OH)^{3+} + H^+ + e^-$$

with an $E^\circ = -1.715$ V (29). An increase in emf occurs on increasing pH from the initial value of 2.5 to 11. This helps oxidation of Ce^{3+} to Ce^{4+}. However, although the high pH shifts the equilibrium, the reaction is still not thermodynamically favored (at pH of 13 an overall thermodynamic constant for the oxidation of Ce^{3+} to Ce^{4+} with dissolved O_2 is $K \sim 10^{-30}$). To drive the equilibrium to the right for complete oxidation of Ce^{3+} to Ce^{4+}, the Ce^{4+} must be withdrawn from the solution, for example, in the form of precipitate. Because of their lower basicity and higher charge, Ce^{4+} ions are easily hydrated to form complexes with OH^- and H_2O ($Ce(H_2O)_x(OH)_y^{(4-y)+}$). Further polymerization and precipitation of these hydroxides to give hydrous oxide and then to the oxide is strongly favored under basic conditions ($K \sim 10^{50}$) and in the presence of the surfactant. Therefore the continuous withdrawal of Ce^{4+} from solution shifts the equilibrium $Ce^{3+/4+}$ in favor of the oxidized state. The occurrence of this process is confirmed by the color changes (colorless → violet → brown → yellow) during reaction, which is consistent with a progressive variation of the redox state of cerium. The violet color is characteristic of poorly defined mixed valence hydrates intermediates which finally give yellow Ce(IV) oxide (30). If surfactant is not added, complete oxidation to Ce(IV) occurs only at the drying stage when the precipitate turns yellow. This observation is also in agreement with previous studies on the behavior of $Ce(NO_3)_3$ under homogeneous precipitating conditions with NH_4OH, where the formation of yellow CeO_2 was detected only after drying (6), whereas in the presence of additional organic oxidants, this oxidation occurred in solution.

The approach we followed can be summarized by the reaction paths outlined in Scheme 2.

The soluble isolated Ce^{3+} under basic conditions oxidizes to a hydrated Ce^{4+} formulated as $Ce(H_2O)_x(OH)_y^{(4-y)+}$, which then incorporates the surfactant in accordance with reaction II. This step can also be viewed as the formation of polymeric hydrous oxide, which then reacts with the alkylammonium salt (steps IIa and IIb) at a pH well above that of the isoelectric point of Ce oxide. Under these conditions,

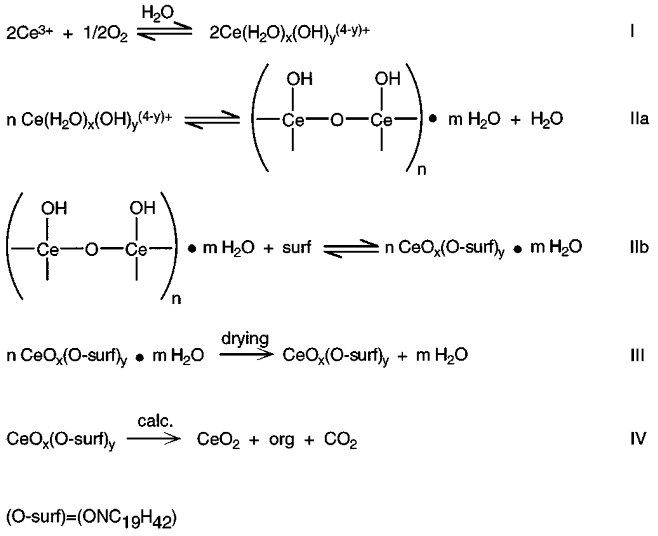

SCHEME 2

an exchange between the deprotonated hydroxy group of the oxide and the alkyl ammonium cation takes place with formation of an inorganic/organic composite which upon drying and calcination (steps 3 and 4) originates pure mesoporous cerium oxide with high surface area. Reaction II determines the amount of organic template which exchanges with the OH groups of the oxide. This depends on pH, reaction time, or the ratio of Ce/surfactant used. We observed that the surfactant is able to promote oxidation of Ce^{3+} to Ce^{4+} and formation of hydrous oxide in solution, before drying. This enhancement can be related to two main causes: (i) the sequestration effected by the surfactant of the species $Ce(H_2O)_x(OH)_y^{(4-y)+}$ (reaction II) and (ii) the number of cerium ions present on the surface of the precipitated particles. In the first case, the surfactant shifts both equilibrium I and II to the right, increasing the amount of exchanged Ce(IV) oxide, while the presence of more surface cerium atoms favorably alters surface energy, and oxidation of Ce^{3+} to Ce^{4+} is more completely directed to Ce^{4+} (12). The presence of more surface cerium atoms is a consequence of the smaller particles formed with the surfactants with a higher number of exposed cerium atoms.

The degree of ordering of our mesoporous ceria, as evidenced in the paper, is poor and limited to some regions only. We believe the failure to provide a mesoscopic organization originates from the redox chemistry of cerium, both in solution and in the solid state, and from the different oxo chemistry of this element in comparison, for example, with elements like Si and Al. We carefully investigated this issue by varying surfactants and reaction conditions (pH, time, temperature, concentration, Ce/C_n ratio) and our conclusion is that a different approach should probably be followed to increase the degree of structural, long range organization. Reduction of Ce^{4+} in high surface area ceria is very easy, so any effort directed at increasing porosity and surface area with a stable and ordered 3D structure will be nullified by a structural collapse due to Ce^{4+} reduction, operated, for example, by the surfactant during drying and calcination.

The questions which remain to be addressed are: (i) why the incorporation of surfactants always results in an enhancement of the surface area of ceria and (ii) why ceria prepared with this methodology has a better thermal stability. The first question could be related to the reduction of the surface tension inside the pores operated by the surfactant during drying and calcination. As the hydrous cerium oxide shrinks, the tension in the pores increases, causing pores to collapse. Surfactant can act by reducing the interfacial energy and thereby decreasing capillary stress, which ultimately has a beneficial effect on pore structure stability. Whether the surfactant can be added at the last stage, before drying, or whether it must be added at the beginning, remains an open question. We have observed that adding the surfactant before drying contributes to the enhancement of surface areas but does not produce the large enhancement observed if the surfactant is incorporated at the start of the process. Most important, resistance to sintering at temperatures between 900 and 1200 K is strongly enhanced by initial incorporation of the surfactant, indicating that the structural arrangement and the morphology of the inorganic–organic material in the hydrogel could also affect performance of the material by affecting the composition of CeO_2/CeO_x phases at increasing temperatures. For example, the higher oxygen storage/transport ability of ceria prepared using surfactants (25) indicates a different O^{2-} migration/diffusion rate and an enhanced stability of nonstoichiometric CeO_{2-x} phases. These features could also contribute to the enhanced textural stability of this ceria in comparison to ceria prepared by conventional precipitation.

CONCLUSIONS

This is to our knowledge the first effort to produce a mesoscopic organization with CeO_2, and the methodology reported here, although failing in providing a long-range ordered three-dimensional structure, allows the preparation of high-surface area ceria, with improved resistance to sintering. This, in turn, allows an enlargement of the temperature window of possible catalytic application of ceria, especially in the treatment of exhaust gases.

ACKNOWLEDGMENTS

The authors are grateful to CNR and MURST for financial support.

REFERENCES

1. Trovarelli, A., *Catal. Rev.-Sci. Eng.* **38**, 439 (1996).
2. Taylor, K. C., "Catalysis, Science and Technology" (J. R. Anderson and M. Boudart, Eds.), p. 119. Springer-Verlag, Berlin, 1984.

3. Schmieg, S. J., and Belton, D. N., *Appl. Catal. B: Environ.* **6**, 127 (1995).
4. Abi-aad, E., Bechara, R., Grimblot, J., and Aboukaïs, A., *Chem. Mater.* **5**, 793 (1993).
5. Bruce, L. A., Hoang, M., Hughes, A. E., and Turney, T. W., *Appl. Catal. A: General* **134**, 351 (1996).
6. Chen, P-L., and Chen, I-W., *J. Amer. Ceram. Soc.* **76**, 1577 (1993).
7. Varma, H. K., Mukundam, P., Warrier, K. G. K., and Damodaran, A. D., *J. Mater. Sci. Lett.* **10**, 666 (1991).
8. Hirano, M., and Kato, E., *J. Amer. Ceram. Soc.* **79**, 777 (1996).
9. Vallet-Regi, M., Conde, F., Nicolopoulos, S., Ragel, C. V., and Gonzales-Calbet, J. M., *Material Science Forum* **235–238**, 291 (1997).
10. Tschöpe, A., and Ying, J. Y., *NanoStruct. Mater.* **4**, 617 (1994).
11. Pijolat, M., Viricelle, J. P., and Soustelle, M., *Stud. Surf. Sci. Catal.* **91**, 885 (1995).
12. Masui, T., Fujiwara, K., Machida, K., Adachi, G., Sakata, T., and Mori, H., *Chem. Mater.* **9**, 2197 (1997).
13. Zhou, Y., Phillips, R. J., and Switzer, J. A., *J. Amer. Ceram. Soc.* **78**, 981 (1995).
14. Perrichon, V., Laachir, A., Abouarnadasse, S., Touret, O., and Blanchard, G., *Appl. Catal. A: General* **129**, 69 (1995).
15. de Leitenburg, C., Trovarelli, A., and Dolcetti, G., *CHEMTECH* **6**, 32 (1997).
16. Cuif, J-P., Blanchard, G., Touret, O., Marczi, M., and Quemere, E., *SAE Paper* 961906, 75 (1996).
17. Kresge, C. T., Leonowicz, M. E., Roth, W. J., Vartuli, J. C., and Beck, J. S., *Nature* **359**, 710 (1992).
18. Hudson, M. J., and Knowles, J. A., *J. Mater. Chem.* **6**, 89 (1996).
19. Reddy, J. S., and Sayari, A., *Catal. Lett.* **38**, 219 (1996).
20. Larsen, G., Lotero, E., Nabity, M., Petkovic, L. M., and Shabe, D. S., *J. Catal.* **164**, 246 (1996).
21. Ciesla, U., Schacht, S., Stucky, G. D., Unger, K. K., and Schüth, F., *Angew. Chem. Int. Ed. Engl.* **35**, 541 (1996).
22. Antonelli, D. M., and Ying, J. Y., *Angew. Chem. Int. Ed. Engl.* **34**, 2014 (1995).
23. Antonelli, D. M., and Ying, J. Y., *Angew. Chem. Int. Ed. Engl.* **35**, 426 (1996).
24. Behrens, P., *Angew. Chem. Int. Ed. Engl.* **35**, 515 (1996).
25. Terribile, D., Trovarelli, A., de Leitenburg, C., Dolcetti, G., and Llorca, J., *Chem. Mater.* **9**, 2676 (1997).
26. Parks, G. A., *Chem. Rev.* **65**, 177 (1965).
27. Johnson, M. F. L., and Mooi, J., *J. Catal.* **103**, 502 (1987). [*J. Catal.* **140**, 612 (1993)]
28. Anderson, J. R., and Pratt, K. C., *in* "Introduction to Characterization and Testing of Catalysts," Academic Press, Australia, 1985.
29. Handbook of Chemistry and Physics, 76th ed., CRC Press, Boca Raton, FL, 1995-1996.
30. Kilbourn, B. T., "Cerium, a Guide to its Role in Chemical Technology," Molycorp Inc., White Plains, NY, 1992.